

PASSAGE THROUGH RESONANCE OF STATICALLY UNBALANCED ROTOR WITH ECCENTRIC AUTOMATIC BALL BALANCER

Cand. Phys.-Math. Sc. Kovachev A.S.

Faculty of Mathematics and Mechanics – St. Petersburg State University, Russia
alex0303@mail.ru

Abstract: Different modes of direct and reverse passage of the resonance region of the statically unbalanced rotor equipped with an imperfectly mounted eccentric ABB (Automatic Ball Balancer) are investigated with the help of the mathematical model. It is shown for the mode of a constant angular acceleration that the maximum amplitude during the reverse passage of the critical region is always lower than the maximum amplitude in the steady-state mode; at the same time the amplitude of whirling in the direct passage, on the contrary, may be greater than the maximum steady-state value. The case of rotor passing through the resonance under the action of a constant external torque was also investigated. The effect of viscous friction in the ABB's cage was studied for both types of modes. The effect of the rapid oscillations of the amplitude caused by the slippage of the balancing balls was discovered in the case of insufficient damping in the ABB.

Keywords: PASSAGE THROUGH RESONANCE, UNBALANCED ROTOR, AUTOMATIC BALL BALANCER

1. Introduction

In works devoted to the study of automatic balancing of rotors with an automatic ball balancer (ABB), it is usually assumed that the center of the ABB lies exactly on the axis of symmetry of the rotor. In practice, these models correspond to ABBs, which are rigidly mounted on the rotors. However, in a number of devices, replaceable ABBs have found application, which are attached to the rotor by means of a threaded connection. For adequate mathematical modeling of this kind of devices, it is necessary to take into account the presence of possible eccentricity between the axes of symmetry of the ABB and the rotor.

The non-stationary motions of unbalanced rotors equipped with ABB were considered in the works [1]-[6]. In [1], the transient processes of establishing balanced modes at constant angular velocity of the rotor were investigated. In [2], the influence of the angular velocity of the rotor on the value of the maximum whirling amplitude in the process of automatic balancing was studied. Numerical methods have shown that a sharp change in the speed of rotation of the rotor can lead to a significant increase of the whirling amplitude. In [3] the synchronous and asynchronous modes of motion of the ABB for the dynamically unbalanced rotor were analytically investigated. In [4], the influence of the mass of balls and friction in the ABB on the modes of nonstationary passage of the critical region at constant angular acceleration of the rotor was studied. It was found that, due to the motion of the balancing balls, the maximum amplitude of the oscillations of the rotor during a nonstationary transition through the critical speed can exceed the maximum amplitude in the stationary case. In [5], nonstationary modes of passage through the critical region for a fixed in elastic orthotropic bearings rotor equipped with an ABB were investigated. In particular, it was noted that in the supercritical region the complete balancing of the rotor in orthotropic bearings is faster than for a similar rotor in isotropic bearings. In [6] it was found that the amplitude of whirling of a rigid rotor with an orthotropically elastic shaft in the "slow" passage mode of the critical region significantly exceeds the whirling amplitude of a similar rotor with an isotropic shaft.

The present work continues the research begun in [7], [8] and is devoted to the study of modes of non-stationary passage through the resonance of a rotor equipped with an ABB, taking into account the imperfection of its mounting.

2. Mechanical model

Fig. 1 presents the rotor model, in the form of a massive hard disk fixed in the middle of a weightless elastic shaft rotating in vertical hinged bearings O_1 and O_2 . It is assumed that the disk is

statically unbalanced, i.e. its center of gravity G does not coincide with the point C of fastening the disk to the shaft.

An automatic ball balancer is installed for compensation of the imbalance and the center E of the circular cavity of the ABB also does not coincide with the point C .

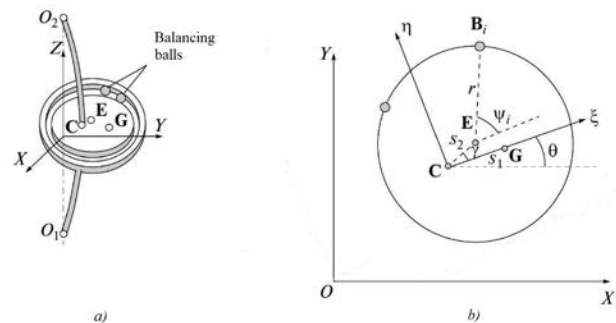


Fig. 1 Rotor with eccentrically mounted ABB.

The presented rotor model with a "non-ideally" mounted ABB is described in [7] and the following notations were introduced: $s_1 = |CG|$ is a static eccentricity of the disk; m_1 is the mass of the disk, m_2 is the mass of the ABB's hull (without balancing balls), m_3 is the mass of one balancing ball; r is the radius of the circular cavity of the ABB; I_G is the central moment of inertia of the disk; k is the coefficient of elasticity of the shaft; c and c_θ are the coefficients of the external viscous resistance to the transverse motion of the rotor and the rotation of the shaft in the bearings; c_ψ is the coefficient of viscous damping in the ABB. Two parameters are introduced for the description of the ABB's eccentricity: the distance s_2 between the points C and E and the angle $\gamma = \angle GCE$.

If the ABB contains n balancing balls, and the disc movement is considered only in the plane of the static eccentricity, then the described system has $n + 3$ degrees of freedom. Choosing the absolute coordinates X and Y of the point C in the fixed system XOY , the angle θ of the rotation of the rotor and the angles of deviation of the balancing balls in the coordinate system $\xi C \eta$ associated with the rotor disk ψ_i ($i = 1, \dots, n$) as generalized coordinates, we write the equations of motion of the system (see [7])

$$m_0 \ddot{X} + c\dot{X} + kX = -\frac{d^2}{dt^2} [m_1 s_1 \cos \theta + (m_2 + n m_3) s_2 \cos(\theta + \gamma) + m_3 r \sum_{j=1}^n \cos(\theta + \psi_j)],$$

$$m_0 \ddot{Y} + c\dot{Y} + kY = -\frac{d^2}{dt^2} [m_1 s_1 \sin \theta + (m_2 + n m_3) s_2 \sin(\theta + \gamma) + m_3 r \sum_{j=1}^n \sin(\theta + \psi_j)],$$

$$J_C \ddot{\theta} + c_\theta \dot{\theta} - c_\psi \sum_{j=1}^n \ddot{\psi}_j = M(t) + m_1 s_1 (\ddot{X} \sin \theta - \ddot{Y} \cos \theta) + (m_2 + n m_3) s_2 (\ddot{X} \sin(\theta + \gamma) -$$

$$\begin{aligned}
 & -\ddot{Y} \cos(\theta + \gamma) - m_3 r s_2 \sum_{j=1}^n ((\dot{\theta} + \dot{\psi}_j)^2 \sin(\gamma - \psi_j) + (\ddot{\theta} + \ddot{\psi}_j) \cos(\gamma - \psi_j)), \\
 & m_3 r^2 (\ddot{\theta} + \ddot{\psi}_j) + c_\psi \dot{\psi}_j = m_3 r (\ddot{X} \sin(\theta + \psi_j) - \ddot{Y} \cos(\theta + \psi_j)) + m_3 r s_2 (\dot{\theta}^2 \sin(\gamma - \psi_j) - \\
 & - \ddot{\theta} \cos(\gamma - \psi_j)), \\
 & j = 1, \dots, n, \tag{1}
 \end{aligned}$$

where

$$\begin{aligned}
 m_0 &= m_1 + m_2 + n m_3, \\
 J_c &= I_G + m_1 s_1^2 + (m_2 + n m_3) s_2^2.
 \end{aligned}$$

The first two equations of (1) describe the motion of the point C in the plane XY. The third equation describes the rotational motion of the rotor. The last n equations describe the motion of the balancing balls.

3. Results and discussion

3.1 Passage of the critical region with constant angular acceleration

We suppose that the motion of the rotor occurs under the action of an energy source ensuring the constancy of its angular acceleration $\ddot{\theta} = b = const$. Then the expressions for the instantaneous angular velocity ω and the rotational angle of the rotor θ take the following form:

$$\begin{aligned}
 \omega(t) &= \dot{\theta} = \omega_0 + bt, \\
 \theta(t) &= \omega_0 t + b \frac{t^2}{2}, \tag{2}
 \end{aligned}$$

where $\omega_0 = \omega(0)$ is the initial angular velocity of the rotor.

We assume further for simplicity that the rotor is equipped with a two-balled ABB. Taking into account (2), the system (1), will be represented by four second-order differential equations. The numerical integration of the system (1) was carried out for the following values of the parameters: $m_1 = 1 \text{ kg}$, $m_2 = 0.2 \text{ kg}$, $\gamma = 0$, $s_1 = 0.003 \text{ m}$, $s_2 = 0.0005 \text{ m}$, $c = 50 \text{ kg/s}$, $c_\psi = 0.1 \text{ kg/s} \cdot \text{m}^2$.

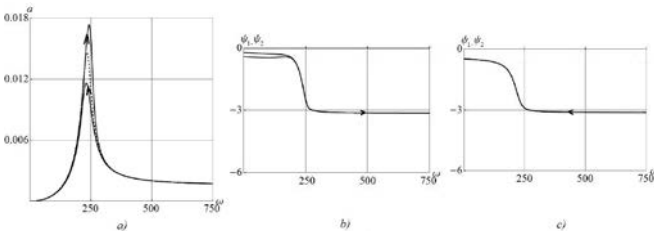


Fig. 2 Direct and reverse passage of the critical region with constant angular acceleration in the case when the mass of the balls is insufficient for the balancing of the rotor.

Fig. 2 presents the results of calculating the direct ($b = 0.25 \text{ s}^{-2}$, $\omega_0 = 0$) and the inverse ($b = -0.25 \text{ s}^{-2}$, $\omega_0 = 1000 \text{ s}^{-1}$) passing through the critical region in the case where the mass of the balancing ball is $m_3 = 0.01 \text{ kg}$. In [7], the following condition was obtained for balancing the rotor: $\sigma = 2 m_3 r / (m_1 + m_2) s_1 > 1$. In our case, this condition is not satisfied, and therefore after passing through the critical region, there is an unbalanced whirling mode.

Fig. 2a shows the amplitude of the whirling motion of the point C as a function of the instantaneous angular velocity ω . The dashed line indicates a stationary amplitude-frequency response. It can be seen from the figure that the maximum amplitude with direct resonance passing exceeds the maximum amplitude of the stationary amplitude-frequency response. This effect is explained by the additional imbalance that arises from the motion of the balls at the moment of transition of the critical region shown in Fig. 2b. In the case of an reverse transition of the critical region, a similar effect does not occur, since the balls in the supercritical region

occupy a position as far as possible from the point O, which minimizes the overall imbalance of the rotor (Fig. 3c).

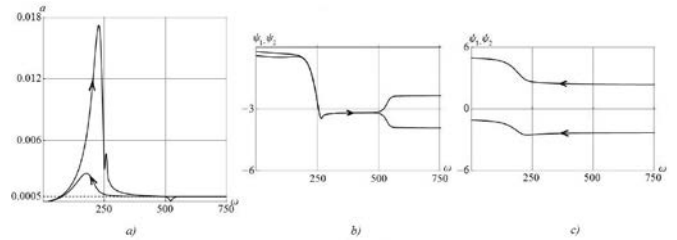


Fig. 3 Direct and reverse passage of the critical region with constant angular acceleration in the case when the mass of the balls is sufficient for the balancing.

Fig. 3 demonstrates the case when the mass of balls is sufficient for balancing ($m_3 = 0.03 \text{ kg}$). The graph in Fig. 3a, which corresponds to the case of a direct passage through the critical region, shows that in the supercritical region a half-balanced mode is being established, whose amplitude is independent of the angular velocity and numerically equals to the value of the ABB's eccentricity indicated by the dotted line. We note that during the transition to a half-balanced mode, the effect of "instantaneous balancing" is observed, when the whirling amplitude rapidly decreases to zero, and then quickly returns to the value corresponding to the half-balanced mode. This effect is explained by the fact that the balls in the process of movement (Fig. 3b) pass through a position which balances the imbalance of the rotor. We also note that the maximum amplitude for the reverse passage is substantially lower than for the direct one, since the balls, as seen from Fig. 3c, initially occupy the best position corresponding to the half-balanced mode.

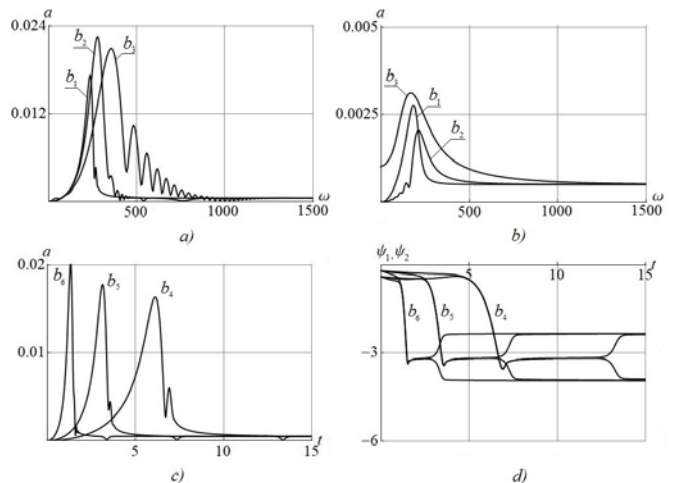


Fig. 4 Passage of the critical region for different angular acceleration values.

To determine the effect of the angular acceleration on the value of the amplitude maximum, calculations are made of the passage of the critical region for various values of the angular acceleration b . Fig. 4a and 4b show the amplitudes of whirling motions for direct and reverse resonance respectively for the following angular acceleration values: $b_1 = 0.25 \text{ s}^{-2}$, $b_2 = 2.5 \text{ s}^{-2}$, $b_3 = 12.5 \text{ s}^{-2}$. We can see from Fig. 4a that for the small values of angular accelerations (i.e. "slow" passage of the critical region), the maximum of the amplitude increases along with the increase in the angular acceleration. However, with a "faster" passage, further growth of the angular acceleration leads to a decrease in the amplitude maximum. The opposite picture is observed in the case of the reverse passage of the critical region (Fig. 4b): for the "slow" passage, the maximum amplitude decreases with increasing acceleration, and increases at a "faster" passage. To explain this phenomenon, let us consider in more detail the case of "slow" passage of the critical region. In Fig. 4c, the time dependences of the direct passage amplitude are presented for the following values

of the parameter b : $b_4 = 0.04 \text{ s}^{-2}$, $b_5 = 0.08 \text{ s}^{-2}$ and $b_6 = 0.2 \text{ s}^{-2}$. The effect of increasing the maximum of the amplitude with increasing angular acceleration is explained by the additional perturbation that arises from the motion of the balancing balls, as shown in Fig. 4d.

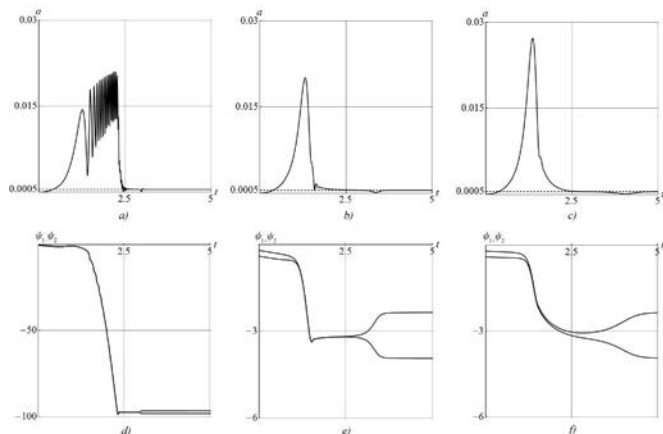


Fig. 5 Effect of the damping coefficient in the ABB.

Let us now investigate the influence of the damping coefficient in the ABB. Fig. 5 shows whirling motion amplitudes and ball angles as a function of time for the case when $b = 0.2 \text{ s}^{-2}$ for three values of the coefficient c_ψ . The graphs show that for $c_\psi = 0.1 \text{ kg / s}\cdot\text{m}^2$ the best auto-balancing mode is achieved (see Fig. 5b and 5e), because in a case of a too small coefficient ($c_\psi = 0.01 \text{ kg / s}\cdot\text{m}^2$), after passing the first resonance peak, rapid oscillations of the amplitude are observed, caused by slipping of the balls in the cage of the ABB (Fig. 5a). This process ends at a certain moment with a "breakdown" of the amplitude and the transition to a half-balanced mode. Too large damping coefficient ($c_\psi = 0.4 \text{ kg / s}\cdot\text{m}^2$) leads to an increase in the maximum value of the whirling amplitude and increases the time required to establish a half-balanced mode (Fig. 5c and 5f).

3.2 Passage of the critical region under the action of constant torque

Let us investigate the motion of the rotor under the action of a constant external torque applied to the disc. Fig. 6 presents the results of the numerical integration of the system (1) for three values of the external torque M . Fig. 6a shows the graph of the amplitude of the whirling motion of the rotor in case when the value of the torque $M = M_1 = 0.03 \text{ N}\cdot\text{m}$ is insufficient for a transition through resonance. The graphs in Fig. 6b are calculated for the values $M_2 = 0.15 \text{ N}\cdot\text{m}$ and $M_3 = 0.27 \text{ N}\cdot\text{m}$. In these cases, the value of the moment is sufficient to pass through the critical region, as a result of which a half-balanced mode is established (the value of the eccentricity of the ABB is indicated by the dotted line). It can be seen from the graph that with increasing torque, the time for establishing a half-balanced mode is shortened. Fig. 6c shows graphs of the rotor's angular velocity variation $\omega = \dot{\theta}$.

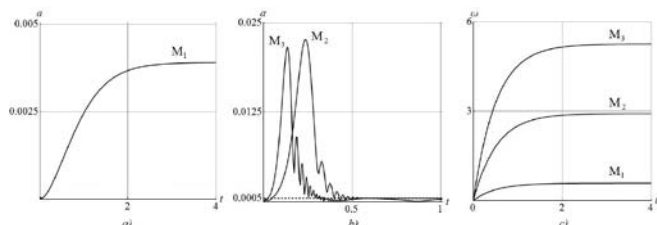


Fig. 6 Passage of the critical region under the action of a constant torque.

Let us consider the case when the rotor is first accelerated by the torque $M = 0.3 \text{ N}\cdot\text{m}$, and then, at $t = t_1 = 1.8 \text{ s}$, the moment becomes zero (Fig. 7c). From Fig. 7a, we see that after passing through the critical region, a half-balanced mode is established. After the torque ceases, the rotor moves in the coasting mode, with the amplitude again beginning to grow, due to the "unbalancing" of the rotor due to the movement of the balancing balls, as shown in

Fig. 7b. The graphs in Fig. 7d - 7f are calculated for a small torque value $M = 0.06 \text{ N}\cdot\text{m}$. The smallness of M , as seen from Fig. 7d, leads to an increase in the time required for the passage of the resonance region, and, as a consequence, leads to an increase in the maximum amplitude of the oscillations. After the torque ceases, the amplitude changes in a manner similar to the previous case.

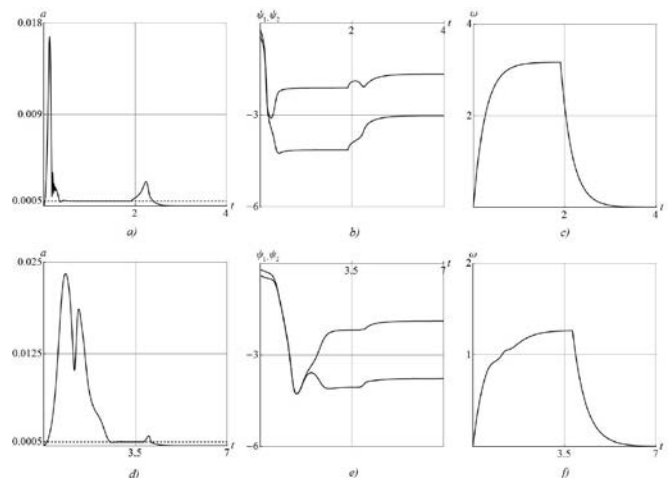


Fig. 7 Motion of the rotor and balancing balls during acceleration and coasting.

Let us now consider the influence of the damping coefficient c_ψ . Fig. 8a - 8c shows the acceleration of the rotor with a small damping coefficient ($c_\psi = 0.004 \text{ kg / s}\cdot\text{m}^2$). As in the case shown in Fig. 5a, fast amplitude oscillations are also observed here due to the sliding of the balls in the cage of the ABB, which end with a "breakdown" and a transition to a half-balanced mode. Fig. 8d - 8f presents the case when at $t = t_1 = 1 \text{ s}$ the applied moment becomes zero. From the graph of the amplitude in Fig. 8d, we see that for $t > t_1$ the average amplitude of the oscillations decreases slowly to zero.

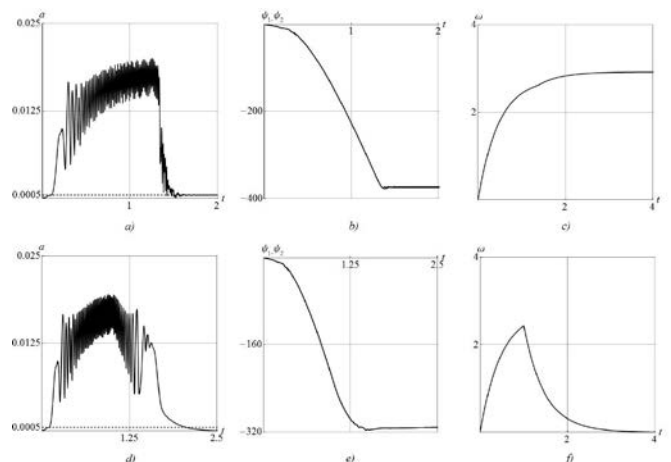


Fig. 8 The effect of slippage of balancing balls in case of insufficient damping in the ABB.

Thus, the comparison of Fig. 3 and 5 with Fig. 7 and 8, respectively, shows that both models similarly describe the non-stationary transition of the rotor with an eccentrically mounted ABB through the critical region.

4. Conclusion

Thus, the calculations above show that the value of the maximum whirling amplitude for a nonstationary transition through the critical speed depends on the angular acceleration and the damping coefficient in the ABB, and in the case of reverse passage, on the magnitude of the additional imbalance introduced by the ABB balls.

References

1. Green K., Champneys A. R. & Friswell M. I. Analysis of the Transient Response of an Automatic Dynamic Balancer for Eccentric Rotors. *International Journal of Mechanical Sciences*, 48(3), March 2006, 274-293.
2. Chung J. Effect of gravity and angular velocity on an automatic ball balancer. *Proceedings of the Institution of Mechanical Engineers, Part C: Journal of Mechanical Engineering Science*, 2005, P. 43-51.
3. Ryzhik B., Sperling L., Duckstein H. Non-synchronous motions near critical speeds in a singleplane auto-balancing device. *Technische Mechanik*. Vol. 24. N1. 2004. P. 25-36.
4. Bykov V.G. Non-stationary modes of motion of a statically unbalanced rotor with an auto-balancing mechanism. *Vestnik St. Petersburg University. Mathematics*, 2010. Vol 3. P. 89-96 [in russian]
5. Bykov V.G. Auto-balancing of rigid rotor in visco-elastic orthotropic bearings. *Vestnik St. Petersburg University. Mathematics*, 2013. Vol 2. P. 82-91. [in russian]
6. Bykov V.G. Auto-balancing of a rotor with an orthotropic elastic shaft. *Journal of Applied Mathematics and Mechanics (English translation of Prikladnaya Matematika i Mekhanika)*, 2013. — Vol. 77, — № 4. — P. 369-379
7. Bykov V.G., Kovachev A.S. Dynamics of a Rotor with an Eccentric BallAutoBalancing Device. *Vestnik St. Petersburg University. Mathematics*, 2014. — Vol. 47, — № No 4. — p. p. 173-180
8. Bykov V.G., Kovachev A.S. On stability of unbalanced steady-state motions of a rotor with eccentric ball autobalancing device. *Mechanics - Seventh Polyakhov's Reading, 2015 International Conference on*; DOI:10.1109/POLYAKHOV.2015.7106720